Since January 2020 Elsevier has created a COVID-19 resource centre with free information in English and Mandarin on the novel coronavirus COVID-19. The COVID-19 resource centre is hosted on Elsevier Connect, the company's public news and information website.

Journal of Environmental Economics and Management 105 (2021) 102401

Contents lists available at ScienceDirect

Journal of Environmental Economics and Management

journal homepage: www.elsevier.com/locate/jeem

Does the COVID-19 lockdown improve global air quality? New cross-national evidence on its unintended consequences☆

Hai-Anh H. Dang [a, b, *], Trong-Anh Trinh [a]

[a] Data Production and Methods Unit, Development Data Group, World Bank, United States
[b] GLO, IZA, Indiana University, Vietnam Academy of Social Sciences, Viet Nam

ARTICLE INFO

Article history:
Received 30 July 2020
Received in revised form 27 November 2020
Accepted 1 December 2020
Available online 10 December 2020

JEL classification:
D00
H00
O13
Q50

Keywords:
COVID-19
Air pollution
Mobility restriction
RDD

ABSTRACT

Despite a growing literature on the impacts of the COVID-19 pandemic, scant evidence currently exists on its impacts on air quality. We offer an early assessment with cross-national evidence on the causal impacts of COVID-19 on air pollution. We assemble a rich database consisting of daily, sub-national level data of air quality for 164 countries before and after the COVID-19 lockdowns and we analyze it using a Regression Discontinuity Design approach. We find the global concentration of NO_2 and $PM_{2.5}$ to decrease by 5 percent and 4 percent, respectively, using data-driven optimal bandwidth selection. These results are consistent across measures of air quality and data sources and robust to various model specifications and placebo tests. We also find that mobility restrictions following the lockdowns are a possible explanation for improved air quality.

1. Introduction

It has by now become clear that the COVID-19 pandemic is not only a global health emergency but has also led to a major global economic downturn. An emerging body of economic literature has examined the negative impacts of COVID-19 on a range of outcomes, but scant evidence currently exists on the impacts of the COVID-19 crisis on air quality.[1] Given the linkage of air pollution to heart and lung damage and other diseases (Brunekreef and Holgate, 2002; Liu et al., 2019), understanding how air quality is affected during the COVID-19 pandemic provides important empirical evidence for health policies, as well as post-pandemic economic policies that involve trade-offs between economic gains and environmental losses.

☆ We would like to thank the editor Nicholas Rivers, two anonymous reviewer, Dean Jolliffe, and Paolo Verme for helpful discussions on earlier versions. Dang would also like to thank the UK Department of International Development for additional funding assistance through a Knowledge for Change (KCP) grant for the World Development Report 2021 "Data for Better Lives". Trinh acknowledges support from the World Bank Young Fellows Program in Forced Displacement.

* Corresponding author. Data Production and Methods Unit, Development Data Group, World Bank, United States.
E-mail addresses: hdang@worldbank.org (H.-A.H. Dang), tronganh.trinh@rmit.edu.au (T.-A. Trinh).

[1] For example, studied topics include unemployment (Fairlie et al., 2020), household consumption (Baker et al., 2020), gender inequality (Dang and Nguyen, 2020), and individual income (loss) and behaviour changes (Akesson et al., 2020).

https://doi.org/10.1016/j.jeem.2020.102401
0095-0696/

The few existing studies focus on country-specific case studies rather than investigate the impacts of the pandemic on the global scale and have yet to offer conclusive evidence. Employing a difference-in-difference model that compares Chinese cities with and without the pandemic-induced lockdown policies, He et al. (2020) find that city lockdowns led to considerable improvement in air quality as measured by Air Quality Index (AQI) and $PM_{2.5}$. This result is consistent with Brodeur et al. (2020) findings for the United States that 'safer-at-home' policies decreased $PM_{2.5}$ emissions. However, using a similar difference-in-difference approach, Almond et al. (2020) show that COVID-19 had ambiguous impacts and might even decrease air quality in Hubei, the province at the center of the outbreak in China. To our knowledge, Lenzen et al. (2020) and Venter et al. (2020) are the only exceptions that examine the pandemic impacts on global air quality. Using an input-output model for 38 regions around the word, Lenzen et al. (2020) find the pandemic to reduce greenhouse gas, $PM_{2.5}$, and air pollutants by 4.6 percent, 3.8 percent and 2.9 percent of the global annual totals, respectively. Comparing air quality during the pandemic with that in previous years, Venter et al. (2020) analyze station-based air quality data in 34 countries and find concentration of NO_2 and $PM_{2.5}$ to decrease by approximately 60 percent and 31 percent.[2]

We add several new contributions to the emerging literature on the pandemic impacts on air pollution. We offer global estimates for the causal impacts of COVID-19 on air quality in 164 countries using a Regression Discontinuity Design (RDD) approach in a short window of time before and after each country implemented its lockdown policies. Since the lockdown policy—as most society-wide regulations—cannot be randomized across countries, the RDD offers us the most rigorous evaluation model that is available. We also provide estimates for several different measures of air quality, including NO_2 and $PM_{2.5}$ (for our main analysis) and O_3, PM_{10}, and SO_2 (for robustness checks). These various indicators help strengthen the estimation results.

Finally, we combine a variety of real-time data sources for richer analysis. We obtain daily data on air pollution at the more disaggregated, sub-national level from satellite data and station-based data. We combine these data with the Oxford COVID-19 Government Response Tracker, a unique database on government policy responsiveness to COVID-19. We supplement our analysis with data from other sources including the National Oceanic and Atmospheric Administration, Google Community Mobility Reports, World Bank World Development Indicators, WHO Global Ambient Air Quality Database, and Economist Intelligence Unit.

The rich database that we assemble allows us to address a key challenge in cross-country analysis, which is to construct comparable lockdown dates for different countries. Indeed, the term 'lockdown' can refer to anything from mandatory quarantines to bans on events and gatherings, businesses closures, or non-mandatory stay-at-home recommendations. Some governments immediately respond to the outbreak by implementing a complete (regional or national) lockdown (e.g., China, Italy), while some implement a gradual lockdown in a staggering manner for different locations (e.g., the United States).

We find strong evidence for reduced air pollution after the lockdowns, with more reduction for a larger window of time around the lockdown dates. In particular, the global decreases in NO_2 and $PM_{2.5}$ hover around 5 percent and 4 percent using the optimal bandwidths of 62 and 88 days after the lockdowns, respectively. We perform various placebo tests and robustness tests using falsified lockdown dates, different indicators of air quality and government policy indexes, alternative bandwidth specifications, functional forms, and inclusion of different covariates.[3] Our findings suggest that mobility restrictions following the lockdowns can be a channel that explains the improvement in air quality.

2. Data

To examine the relationship between COVID-19 and air quality, we use two measures of air pollution, namely fine particulate matter $PM_{2.5}$ (mass concentration of particles with diameters $\leq$2.5 μm) and nitrogen dioxide NO_2. $PM_{2.5}$ is a common cause for adverse health outcomes such as chronic obstructive pulmonary disease and lower respiratory infection causing death of nearly three million people globally (Gakidou et al., 2017). At the same time, NO_2 is the leading source of childhood asthma in urban areas (Achakulwisut et al., 2019).

We obtain high-resolution global NO_2 data from the Sentinel-5P/TROPOMI (S5P) instrument of the European Union's Copernicus programme. As an alternative air-quality measure, we use daily station-based air quality index (AQI) from the World Air Quality Index (WAQI) project. However, given certain limitations with station-based data (such as slower reporting and likely non-random locations), the satellite data are our preferred data for analysis. Finally, we obtain sub-national data on daily rainfall and temperature from the National Center for Environmental Prediction (NCEP) at the National Oceanic and Atmospheric Administration (NOAA).

We subsequently merge the air pollution data with the government stringency data from the Oxford University's COVID-19 Government Response Tracker (OxCGRT), which contains information on various lockdown measures, such as school and

[2] A recent study applies time series analysis to historical data to predict the impacts of pandemic on air pollution (Smith et al., 2020). Other studies examine instead the related impacts on health outcomes caused by the pandemic-induced changes in air quality (Cicala et al., 2020; Cole et al., 2020; Isphording and Pes·tel, 2020).

[3] We also find some limited evidence that countries with a higher share of trade and manufacturing in the economy have more reduced air pollution after the lockdowns, as do countries with an initially lower level of air pollution. But the opposite result holds for countries near the equator (see Appendix C).

workplace closings, travel restrictions, bans on public gatherings, and stay-at-home requirements (Hale et al., 2020). The OxCGRT data measure government stringency responses on a scale of 0–100.

To explore a potential channel through which COVID-19 affects air quality, we collect data on global mobility from Google Community Mobility Reports (GCMR). The GCMR provide daily mobility data in different categories on Google Maps users across 132 countries. We provide a more detailed description of the data sources and the summary statistics of the main variables in Appendix B, Table B1.

3. Empirical model

We first employ for analysis the following fixed-effects panel data model

$$A_{it} = \beta S_{it} + \gamma X_{it} + \alpha_i + \tau_t + \varepsilon_{it} \quad (1)$$

The coefficient of interest in Equation (1) is β, which measures how the air quality (A_{it}) in country i and date t changes in response to the stringency of government COVID-19 policies (S_{it}). Because S_{it} varies by country and date, this fixed-effects model allows for the inclusion of country fixed effects (α_i) and time fixed effects (τ_t) to absorb the effects of unobservable time-invariant country or time characteristics. X_{it} is a vector of observed time-varying control variables such as daily temperature and rainfall.

Yet, Equation (1) yields an inconsistent estimate of β if omitted variables exist that correlate with both air quality and government policies. Since S_{it} is positive only after the lockdown date, Equation (1) does not address the fact that unobserved pre-COVID-19 time-varying country characteristics, such as governance quality and public preferences for protecting the environment, can differ. Another challenge in this context is that air pollution is positively associated with the number of COVID-19 cases (Cicala et al., 2020; Cole et al., 2020; Isphording and Pestel, 2020), which can lead to governments implementing more stringent lockdown. Failure to control for possible reverse causality would result in biased estimates of the effects of the lockdown.

We propose two strategies in this paper to identify the causal effects of COVID-19 on air quality. First, we use a flexible event study framework to help mitigate concerns about the common trends. Specifically, we decompose the estimated effects of lockdown (S_{it}) into coefficients up to 100 days prior to and following the lockdown date. This will provide a descriptive test for whether the lockdowns are correlated with differential trends before and after the lockdowns. Second, we apply a more rigorous econometric technique by taking advantage of the pandemic-induced lockdowns as an exogenous policy shock and applying a Regression Discontinuity Design in Time (RDiT) approach. In this approach, the observations immediately before the lockdown dates provide the counterfactual outcomes for those observations immediately after the lockdown dates because the lockdown (treatment) status is randomized in a small neighborhood of the lockdowns. This approach is built on the standard Regression Discontinuity Design (RDD) (see, e.g., Hahn et al. (2001)) but the running variable is the days from the lockdown dates. It has been widely used in the literature to study changes in air quality caused by a specific event (Davis, 2008; Auffhammer and Kellogg, 2011; Chen and Whalley, 2012). We estimate the following reduced form

$$A_{it} = \delta L_{it} + f(d_{it}) + \theta X_{it} + \mu_i + \pi_t + \varepsilon_{it} \quad (2)$$

where L_{it} (treatment variable) is a dummy variable that equals 1 after the lockdowns and 0 otherwise, and δ is the parameter of interest. $f(d_{it})$ denotes a function of the running variable d_{it} (number of days from the lockdown dates). Similar to Equation (1), μ_i and π_t respectively denote the country fixed effects and the time fixed effects, and ε_{it} denotes the error term. For comparison and robustness checks, we use different functional forms of the running variable d_{it} to estimate Equation (2). These include (i) the linear model (d_{it}), (ii) the linear model with the interaction term of the running variable and the treatment variable ($L_{it}{*}d_{it}$), (iii) the quadratic model (d_{it}^2), and (iv) the quadratic model with the interaction term of the running variable and the treatment variable ($L_{it}{*}d_{it}^2$).[4] Since our estimates might be sensitive to bandwidth choices, we employ Imbens and Kalyanaraman (2012)'s data-driven selection procedures to obtain the optimal bandwidths.

As discussed earlier, a key challenge with estimating Equation (2) is to identify lockdown dates that are comparable across different countries, which likely implement lockdowns with various degrees of strictness. For example, business activities and travels can continue to varying extents after the lockdown dates, or while all schools are shut down, universities operate on a different schedule for different countries. Furthermore, there can be multiple lockdown dates even within the same country where regions/states impose different lockdown dates (with different levels of intensity). To address this issue, the OxCGRT provides a unique composite measure which combines indicators on different aspects of lockdown policies regarding school, workplace, public transportation, and public events into a general index (Appendix B, Table B2). By using a range of different indicators, this stringency index accounts for any indicator that may be over- or mis-interpreted, thus allows for a better and more systematic comparison across countries (Hale et al., 2020).

[4] We offer additional results using high-order polynomial terms in Table A6 (Appendix A); however, controlling for high-order polynomials in RDD analysis may lead to noisy estimates (Gelman and Imbens, 2019).

For each country, we define the lockdown date as the first day on which the stringency index becomes positive. Using our constructed measure, Figure A1 (Appendix A) shows that most countries introduced lockdowns somewhere between the last week of January and the first week of February 2020, and countries that implemented lockdown policies later tend to have more stringent responses.[5]

To validate the RDD identifying assumptions, we present two types of tests. First, we conduct a discontinuity test in the covariates, namely temperature and precipitation, around the lockdown dates. The results, presented in Table A1 (Appendix A), show no discontinuity at the cut-off date. This finding is further confirmed by Figure A2 (Appendix A). Second, another concern with the RD-in-time approach is serial correlation (Hausman and Rapson, 2018). To address this issue, we follow previous studies and cluster the standard errors on both the location and time dimensions (Auffhammer and Kellogg, 2011; Anderson, 2014). Furthermore, we conduct a robustness check by including the lagged dependent variable in the regressions and find consistent results with our main findings (see Table A2, Appendix A).

4. Results

4.1. Main findings

We present in Table 1 the estimation results for Equation (1) using data at the sub-national level (columns 1 and 2) and the country level (columns 3 and 4). Our preferred results are columns (2) and (4), which control for daily temperature and precipitation (humidity for station-based data).[6] But we also show the estimates without these control variables in columns (1) and (3) for comparison and robustness checks. The estimation results are strongly statistically significant in our preferred models (columns 2 and 4) and point to reduced air pollution where government policies are more stringent. Overall, our findings suggest that global air quality improved in response to COVID-19-induced lockdown policies.

Column (2) indicates that a one-point increase in the stringency index is associated with a 0.012 mol/km^2 (mole per square kilometer) decrease in NO_2 (Panel A). The corresponding figure for station-based data is a 0.129 μg/m^3 (micogram per cubic meter) decrease in $PM_{2.5}$ (Panel B). Estimates at the country level (column 4) are similar to those at the sub-national level (column 2). However, as discussed earlier, the estimates based on Equation (1) are likely biased since they do not properly account for the unobservables that may correlate with both the stringency index and air quality.

To address this issue, we conduct time-event analysis by regressing air quality on a full set of control variables and location and time fixed effects, and a series of "event time" indicators. These indicator variables are in groups of 10 days for days

Table 1
Government response to COVID-19 and air pollution.

	ADM1/City level		Country level	
	(1)	(2)	(3)	(4)
Panel A: Air quality is measured by NO_2 (satellite data)				
Stringency index	−0.032***	−0.012***	−0.040***	−0.033***
	(0.003)	(0.003)	(0.004)	(0.004)
Controls	No	Yes	No	Yes
Country and time FE	Yes	Yes	Yes	Yes
Observations	250,838	248,120	14,850	14,712
Panel B: Air quality is measured by $PM_{2.5}$ (station-based data)				
Stringency index	−0.164***	−0.129***	−0.175***	−0.148***
	(0.016)	(0.016)	(0.011)	(0.011)
Controls	No	Yes	No	Yes
Country and time FE	Yes	Yes	Yes	Yes
Observations	81,478	75,048	12,784	11,986

Notes: ***p < 0.01, **p < 0.05, *p < 0.1. Results of panel model. Clustered standard errors in parentheses are robust to within-day and within-country serial correlation. Control variables are daily temperature and rainfall (humidity for station-based data).

[5] Although the OxCGRT data provides a systematic comparison across different countries, it is still possible that not all business activities and travel cease exactly by the time of our constructed lockdown dates. In that case, a better approach is to employ the fuzzy RDD model rather than the sharp RDD model where the treatment variable L_{it} can assume the value of 0 for $S_{it} > 0$ for some countries. However, we do not have such additional information for L_{it} in our case and have to uniformly define L_{it} as 1 after the lockdown date for each country. But we offer a multi-layered approach to ensure that estimation results are robust. First, the estimates using Equation (1) above provide the first set of evidence over the (correlational) relationship between air quality and the government stringency index. Second, examining the outcomes over several different time bandwidths helps average out any lingering impacts after the lockdowns and provides comparisons. The subsequent estimates remain (qualitatively) similar, indicating that they are robust to this concern. Third, estimates also remain robust to different ways to aggregate data (such as using weekly air quality data instead of daily air quality data) and different versions of the stringency index (such as probing more deeply into its different components). Finally, we also offer a battery of other additional robustness tests in Section 4.2.

[6] Precipitation from the station-based data is not used due to its low frequency.

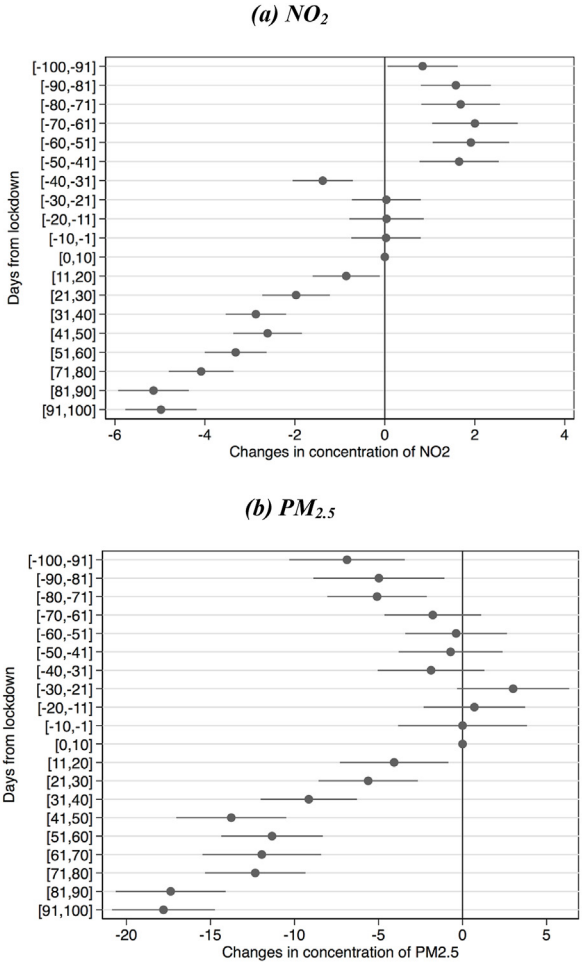

Notes: Figure reports effects of lockdowns and confidence intervals from time-event analysis, with location and time fixed effects. In Panel A, air pollution is measured by concentrations of NO_2 from satellite data. In Panel B, air pollution is measured by concentrations of $PM_{2.5}$ from station-based data. Control variables are daily temperature and rainfall (humidity for station-based data). The reference group is 10 days after the lockdown date.

Fig. 1. Event study analysis. *Notes:* Figure reports effects of lockdowns and confidence intervals from time-event analysis, with location and time fixed effects. In Panel A, air pollution is measured by concentrations of NO_2 from satellite data. In Panel B, air pollution is measured by concentrations of $PM_{2.5}$ from station-based data. Control variables are daily temperature and rainfall (humidity for station-based data). The reference group is 10 days after the lockdown date.

ranging from −100 to +100 before and after the lockdown dates. Fig. 1 plots these results, which confirm our previous finding that concentrations of air pollution are significantly lower after the lockdown dates (Panels A and B), and the impacts are more pronounced for satellite data (Panel A).

We subsequently present the main estimation results using our preferred identification – the RD-in-time model. We start first with showing in Fig. 2 the prima facie evidence of the impacts of lockdowns on air quality. The figure plots the residuals from a data-driven RDD regression of air pollution, measured by NO_2 (Panel A) and $PM_{2.5}$ (Panel B), on daily temperature and rainfall against the days before and after the lockdown dates. A negative jump at the lockdown (cut-off) dates suggests reduced air pollution after the lockdowns. The downward sloping trend for air pollution in Fig. 2 also suggests that the reduction in air pollution becomes stronger as the lockdowns go into effect for a longer period. This is understandable, since a short period of time may not be sufficient to detect the changes in air quality.[7]

We report the estimation results for Equation (2) in Table 2, which shows estimates using two data samples: the satellite data (Panel A) and the station-based data (Panel B). Our preferred models are, again, those that control for weather conditions

[7] We replicate the graphical analysis in Fig. 2 for several countries from different regions. The results (Appendix A; Figure A3) confirm our expectation that the lockdowns result in significant reduction of air pollution.

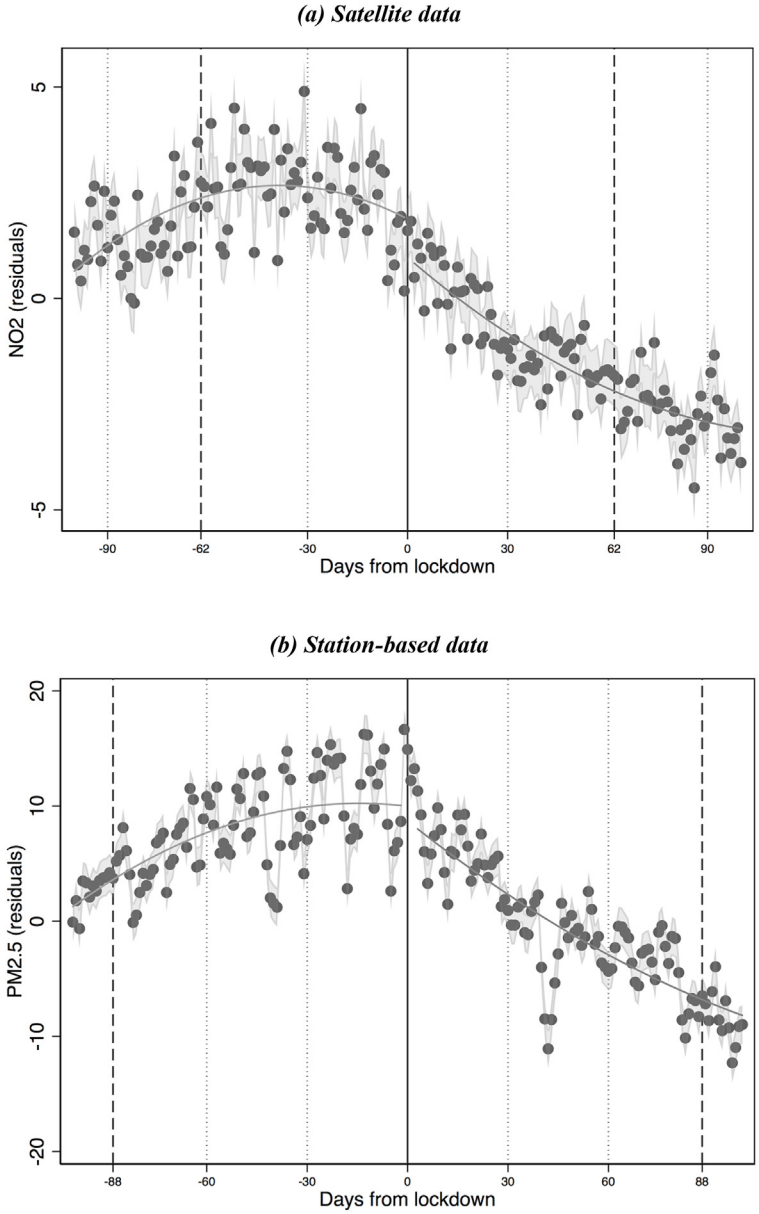

Notes: In Panel A, air pollution is measured by concentrations of NO_2 from satellite data. In Panel B, air pollution is measured by concentrations of $PM_{2.5}$ from station-based data. The continuous line is the predicted outcomes from the RDD regression using the optimal bandwidths based on Imbens and Kalyanaraman (2012). The optimal bandwidths are shown in dash lines.

Fig. 2. COVID-19 lockdowns and air pollution. *Notes:* In Panel A, air pollution is measured by concentrations of NO_2 from satellite data. In Panel B, air pollution is measured by concentrations of $PM_{2.5}$ from station-based data. The continuous line is the predicted outcomes from the RDD regression using the optimal bandwidths based on Imbens and Kalyanaraman (2012). The optimal bandwidths are shown in dash lines.

(columns 2, 4, and 6). We use the optimal data-driven bandwidth selection procedures proposed by Imbens and Kalyanaraman (2012).[8] The estimation results using the satellite data, our main data for analysis, show that air quality

[8] We also plot the estimated impacts of lockdowns for other bandwidths that range from 0 to 100 days. The estimation results, shown in Figure A4 (Appendix A), indicate that the lockdown impacts become much weaker for bandwidths of up to 50 and 80 days for satellite and station-based data, respectively.

Table 2
COVID-19 lockdowns and air pollution.

Panel A: Satellite air pollution Air quality:	Optimal bandwidth		Optimal bandwidth +10 days		Optimal bandwidth −10 days	
NO_2	(1)	(2)	(3)	(4)	(5)	(6)
Model 1: Linear model						
Lockdown = 1	−1.251***	−1.260***	−1.482***	−1.512***	−0.898**	−0.918***
	(0.326)	(0.321)	(0.314)	(0.310)	(0.354)	(0.348)
Model 2: Linear interaction model						
Lockdown = 1	−1.227***	−1.230***	−1.462***	−1.494***	−0.865**	−0.871**
	(0.324)	(0.319)	(0.312)	(0.307)	(0.352)	(0.346)
Model 3: Quadratic model						
Lockdown = 1	−1.242***	−1.251***	−1.480***	−1.520***	−0.877**	−0.888**
	(0.325)	(0.320)	(0.313)	(0.307)	(0.353)	(0.346)
Model 4: Quadratic interaction model						
Lockdown = 1	−1.227***	−1.235***	−1.470***	−1.508***	−0.863**	−0.874**
	(0.326)	(0.321)	(0.314)	(0.309)	(0.353)	(0.347)
Means before lockdowns	23.281	23.281	23.281	23.281	23.281	23.281
Controls	No	Yes	No	Yes	No	Yes
Country and time FE	Yes	Yes	Yes	Yes	Yes	Yes
Observations	260,007	257,339	303,316	300,266	216,917	214,775
Panel B: Station-based air pollution Air quality:	Optimal bandwidth		Optimal bandwidth +10 days		Optimal bandwidth −10 days	
$PM_{2.5}$	(1)	(2)	(3)	(4)	(5)	(6)
Model 1: Linear model						
Lockdown = 1	−4.406***	−2.525**	−4.790***	−2.713**	−3.954***	−1.998
	(1.107)	(1.257)	(1.105)	(1.235)	(1.181)	(1.314)
Model 2: Linear interaction model						
Lockdown = 1	−3.830***	−2.049*	−4.149***	−2.284*	−3.433***	−1.584
	(1.067)	(1.225)	(1.049)	(1.196)	(1.136)	(1.280)
Model 3: Quadratic model						
Lockdown = 1	−3.976***	−2.133*	−4.303***	−2.396**	−3.568***	−1.662
	(1.078)	(1.240)	(1.063)	(1.211)	(1.148)	(1.297)
Model 4: Quadratic interaction model						
Lockdown = 1	−3.805***	−2.035*	−4.143***	−2.231*	−3.375***	−1.599
	(1.059)	(1.217)	(1.047)	(1.188)	(1.128)	(1.269)
Means before lockdowns	64.824	64.824	64.824	64.824	64.824	64.824
Controls	No	Yes	No	Yes	No	Yes
Country and time FE	Yes	Yes	Yes	Yes	Yes	Yes
Observations	90,938	79,200	100,869	89,117	80,962	69,238

Notes: ***p < 0.01, **p < 0.05, *p < 0.1. Results of RDD using the optimal bandwidths based on Imbens and Kalyanaraman (2012). The optimal bandwidths are 62 and 88 days for satellite and station-based data, respectively. Clustered standard errors in parentheses are robust to within-day and within-country serial correlation. Model 1 uses running variable in linear form, Model 2 includes interaction of running variable and treatment variable, Model 3 includes quadratic term of running variable, Model 4 includes interactions of running variable (linear and quadratic terms) with treatment variable. Control variables are daily temperature and rainfall (humidity for station-based data).

improves after the lockdowns, and the results are strongly statistically significant at the 5 percent level or less (Panel A). The estimates are qualitatively similar whether we include the control variables.

Specifically, the estimated coefficient on the lockdown variable is negative and statistically significant at the 1 percent level using the linear model (Panel A, column 2), indicating that the lockdown leads to a 1.260-mol/km^2 decrease in the global concentration of NO_2 using the optimal bandwidth of 62 days. This translates into a 5.4-percent decrease compared to an average value of NO_2 of 23.281 mol/km^2 before the lockdowns. Using different functional forms (models 2 to 4) results in similar estimates. Finally, we present the results using different bandwidth lengths (±10 days from the optimal bandwidth) and find consistent impacts of the lockdowns on NO_2. The decreases in concentration of NO_2 are roughly 6.5 percent for 72 days (Panel A, column 4) and 3.9 percent for 52 days (Panel A, column 6) after the lockdowns.

We turn next to the alternative station-based data. Using the optimal bandwidth of 88 days, we find that the global decrease in $PM_{2.5}$ hovers around 3.1 to 3.9 percent depending on the functional form that we employ (Panel B, column 2). These results are consistent with the global reduction of 4 percent in $PM_{2.5}$ estimated by Lenzen et al. (2020). But estimates become statistically insignificant for the narrower bandwidth of 78 days.[9]

We now perform a set of placebo tests to check the robustness of our results, as reported in Table 3. First, we falsely assume the cut-off date to be 5, 10, 15, 30, and 45 days prior to the lockdown dates. Regardless of measures of air pollution, the

[9] Using different measures of air pollution available from the station-based data yields a similar conclusion (Table A3, Appendix A). An exception is the indicator O_3 which is found to be positively associated with the lockdowns. A possible explanation for the increase in concentration of O_3 is warmer weather during this period (Tobías et al., 2020).

Table 3
Placebo test.

Dependent variable:	NO_2	$PM_{2.5}$
	(1)	(2)
Panel A: 5 days prior to lockdown date		
Lockdown = 1	−1.193*	−1.257
	(0.656)	(2.479)
Observations	256,246	79,098
Panel B: 10 days prior to lockdown date		
Lockdown = 1	−0.894	0.517
	(0.593)	(2.442)
Observations	255,785	78,918
Panel C: 15 days prior to lockdown date		
Lockdown = 1	−0.300	2.714
	(0.555)	(2.505)
Observations	254,805	78,415
Panel D: 30 days prior to lockdown date		
Lockdown = 1	0.043	2.719
	(0.449)	(3.603)
Observations	253,870	76,384
Panel E: 45 days prior to lockdown date		
Lockdown = 1	0.533	−0.751
	(0.763)	(1.798)
Observations	252,852	71,773
Panel F: China lockdown date		
Lockdown = 1	0.489	−1.429
	(0.623)	(1.474)
Observations	252,003	78,463
Panel G: India lockdown date		
Lockdown = 1	−0.049	−1.811
	(0.450)	(1.107)
Observations	252,306	78,594
Means before lockdowns	23.281	64.824
Controls	Yes	Yes
Country and time FE	Yes	Yes

Notes: ***p < 0.01, **p < 0.05, *p < 0.1. Results of RDD using the optimal bandwidths based on Imbens and Kalyanaraman (2012). The optimal bandwidths are 62 and 88 days for satellite and station-based data, respectively. Clustered standard errors in parentheses are robust to within-day and within-country serial correlation. Control variables are daily temperature and rainfall (humidity for station-based data).

treatment effects are not statistically significant (Panels A to E). Second, we use the lockdown dates of several countries as placebo tests, which is motivated by the fact that the shutdown of a large trading economy partner may have spill-over effects on local industrial activity, and thereby affecting air pollution. We select China and India given their large economies and trade resources. Again, the statistically insignificant results lend support to our main specification (Panels F to G). Finally, following Barreca et al. (2011), we also conduct a "donut" RDD by systematically removing observations 5 and 10 days near the lockdown dates. This approach allows us to address potential anticipation effects around the lockdown dates (i.e., there is non-random sorting around the threshold). The results, presented in Table A4 (Appendix A), rule out this concern.

4.2. Further robustness tests and heterogeneity analysis

We conduct a battery of robustness tests on the estimation results. These include employing different procedures for selecting the optimal bandwidth, higher-degree polynomials of the running variable, adding different covariates to the regressions (i.e. such as GDP per capita in constant 2010 USD, population density, log of energy consumption per capita, the number of motor vehicles per 1000 inhabitants, and the share of electricity generated by coal power), using wider time bandwidths (i.e., weekly indicators) and different versions of the stringency index, controlling for potentially differential time

Table 4
Stringency index and mobility restriction.

Mobility changes	Retail and recreation	Grocery and pharmacy	Park	Transit	Workplaces	Residential
	(1)	(2)	(3)	(4)	(5)	(6)
Panel A: Sub-national level						
Stringency index	−0.820***	−0.392***	−0.587***	−0.772***	−0.624***	0.292***
	(0.014)	(0.020)	(0.012)	(0.012)	(0.013)	(0.004)
Controls	Yes	Yes	Yes	Yes	Yes	Yes
Country and time FE	Yes	Yes	Yes	Yes	Yes	Yes
Observations	377,883	364,427	225,097	258,844	471,734	267,863
Panel B: Country level						
Stringency index	−0.766***	−0.481***	−0.539***	−0.789***	−0.596***	0.285***
	(0.005)	(0.005)	(0.007)	(0.004)	(0.005)	(0.002)
Controls	Yes	Yes	Yes	Yes	Yes	Yes
Country and time FE	Yes	Yes	Yes	Yes	Yes	Yes
Observations	13,284	13,284	13,284	13,284	13,284	13,238

Notes: ***p < 0.01, **p < 0.05, *p < 0.1. Results of panel model. Clustered standard errors in parentheses are robust to within-day and within-country serial correlation. Control variables are daily temperature and rainfall.

trends across countries, and converting the air quality variables into the logarithmic form. The estimation results, which are presented in Appendix A, Tables A6 to A13 and discussed in detail in Appendix C, remain robust.

We further examine whether the impacts of lockdowns differ by country characteristics. Estimation results, shown in Table A14 (Appendix A), suggest that after the lockdowns i) countries near the equator have a higher concentration of NO_2, ii) countries with strong institutions do not perform better in terms of air quality, iii) countries with a larger share of trade or manufacturing have more reduced air pollution, and iv) countries with an initially lower level of air pollution (i.e., the 1st quintile) have more reduced air pollution compared to those with initially higher levels of air pollution. Several countries with a large population size that recorded higher air quality stand out, including China, Iraq, Norway, Russia, South Korea, and the United States (see Figure A5; Appendix A).

4.3. Stringent policies and mobility restriction

Once we established the causal impacts of COVID-19 on air pollution, we shift our attention to the role of mobility restrictions as a potential mechanism. Since one main source of air pollution comes from traffic mobility (Viard and Fu, 2015), more stringent policies can result in less mobility, thereby improving air quality. We directly test this hypothesis, using data from the Google Community Mobility Reports. Since mobility data were not available before the lockdown date, we are unable to apply the more rigorous RDD approach. We thus present in Table 4 the estimation results using the fixed-effects model in Equation (1), which show that human mobility has declined significantly where government policies are more stringent.[10] In particular, a higher stringency index is associated with less mobility in both 'essential services' (e.g., grocery and pharma, workplace) and 'non-essential services' (retail and recreation, parks), but more mobility in the 'residential' category.

5. Conclusion

We offer an early study that provides cross-national evidence on the causal impacts of COVID-19 on air pollution. We assemble a rich database from various sources, which we analyze with RDD and panel data models. We find the COVID-19-induced lockdowns to result in significant decreases in global air pollution. Results of placebo tests reassure that our findings are not driven by confounding factors. We also find heterogeneous impacts for different country characteristics, and we identify reduced mobility, especially nonessential individual movements, as a potential channel that can help improve air quality on a global scale. A promising direction for future research is to identify ways to maintain these beneficial impacts on air quality (e.g., through reduced mobility) when the economy returns to pre-COVID-19 conditions.

[10] The Google Community Mobility Reports starts collecting data on mobility data from February 15th, 2020. We estimate that about 109 countries (out of 164) have already implemented lockdowns based on the stringency index. The estimation results obtained by the panel data model (Table 1) are qualitatively similar to those obtained by the RDD approach (Table 2), suggesting that applying this model can provide some qualitative evidence on the mechanism of impacts.

Appendix A. Additional Figures and Tables

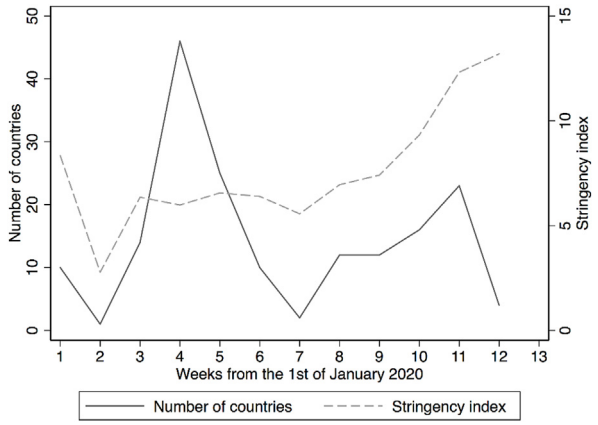

Fig. A1. Number of countries that introduced lockdowns and average policy stringency index.

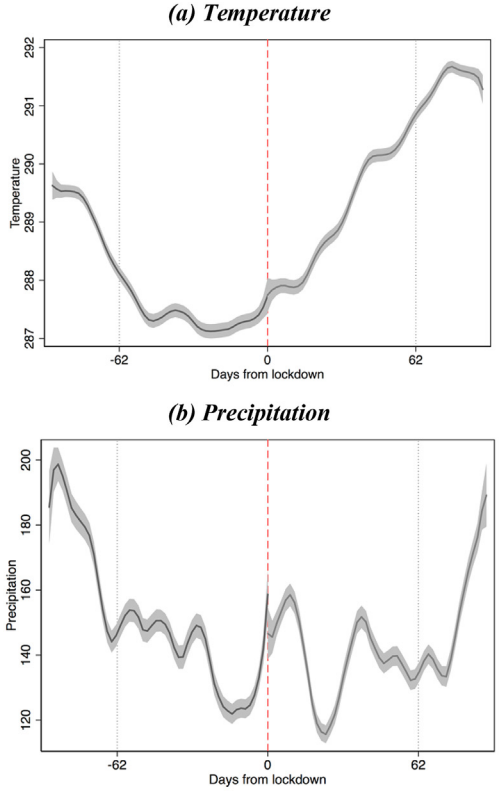

Notes: Temperature and precipitation data are derived from the National Center for Environmental Prediction (NCEP) at the National Oceanic and Atmospheric Administration (NOAA). The continuous line is the predicted outcome from RDD regression using the optimal bandwidths based on Imbens and Kalyanaraman (2012). The optimal bandwidths are shown in dash lines.

Fig. A2. COVID-19 lockdowns and temperature/precipitation.

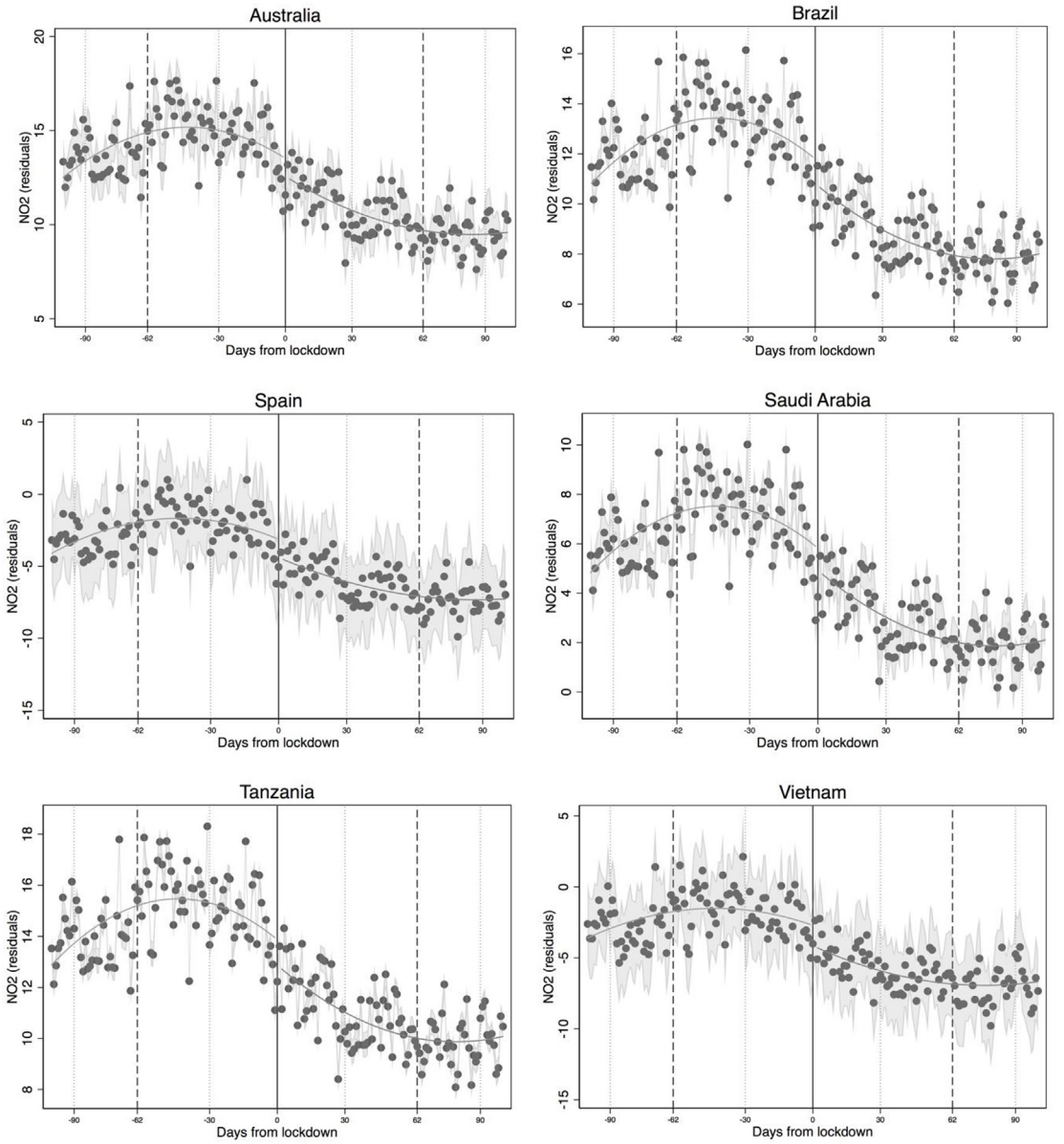

Notes: Air pollution is measured by concentrations of NO_2 from satellite data. The continuous line is the predicted outcomes from the RDD regression using the optimal bandwidths based on Imbens and Kalyanaraman (2012). The optimal bandwidths are shown in dash lines.

Fig. A3. COVID-19 lockdowns and air pollution – Country-specific case studies.

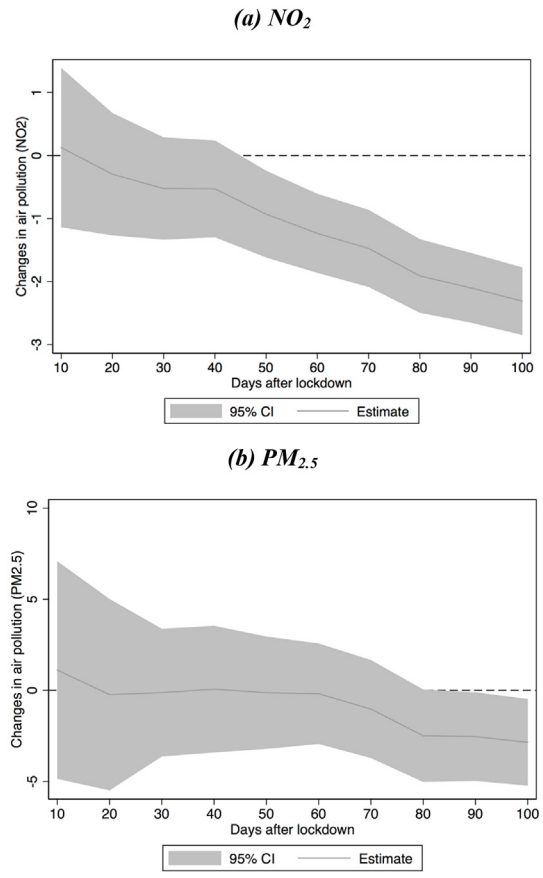

Notes: Air pollution is measured by NO_2 from satellite data (panel a) and $PM_{2.5}$ from station-based data (panel b). Each point in the figure shows point estimate and 95 percent confidence interval of treatment variable (lockdown) using different bandwidths after the lockdown. The parametric RDD model includes interactions of running variable (linear and quadratic terms) with treatment variable. The running variable is number of days from the lockdown date. All regressions include location dummies and time dummies. Control variables are daily temperature and rainfall (humidity for station-based data).

Fig. A4. COVID-19 lockdowns and air pollution – Alternative bandwidths.

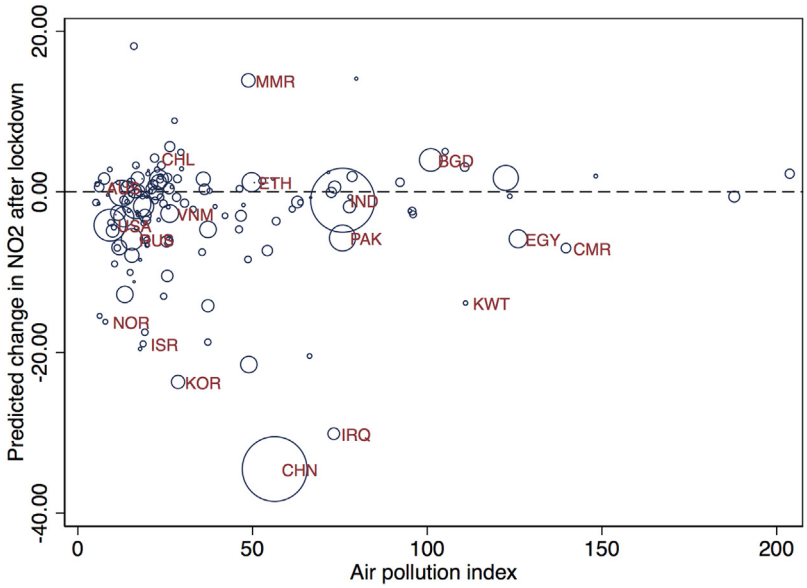

Notes: Air index is measured by concentration of $PM_{2.5}$ at country level from the 2018 WHO Global Ambient Air Quality Database, where a higher index indicates a higher level of pollution. The figure shows the point estimates of the interaction of the treatment variable (lockdown) and the country dummies using RDD model. The running variable is the number of days from the lockdown date. The optimal bandwidths are based on Imbens and Kalyanaraman (2012). Countries are depicted with their population sizes taken from 2019 WDI database. Control variables are daily temperature and rainfall.

Fig. A5. Air pollution reduction by country.

Table A1
Lockdown impacts on weather conditions.

Dependent variable:	Temperature	Rainfall
	(1)	(2)
Lockdown = 1	0.752	−0.002
	(0.742)	(0.014)
Controls	Yes	Yes
Country and time FE	Yes	Yes
Observations	425,624	425,624

Notes: ***p < 0.01, **p < 0.05, *p < 0.1. Results of RDD. Clustered standard errors in parentheses are robust to within-day and within-country serial correlation. The optimal bandwidths are calculated based on Imbens and Kalyanaraman (2012). Control variable in columns (1) and (2) is daily rainfall and temperature, respectively.

Table A2
COVID-19 lockdowns and air pollution − Lagged dependent variable estimation.

Bandwidth	Air pollution: NO_2			Air pollution: $PM_{2.5}$		
	Optimal bandwidth	Optimal bandwidth +10 days	Optimal bandwidth −10 days	Optimal bandwidth	Optimal bandwidth +10 days	Optimal bandwidth −10 days
Lockdown = 1	−0.421***	−0.552***	−0.208*	−0.639**	−0.586**	−0.520
	(0.125)	(0.121)	(0.115)	(0.311)	(0.286)	(0.332)
Lagged dependent variable	0.646***	0.648***	0.628***	0.707***	0.719***	0.696***
	(0.026)	(0.025)	(0.027)	(0.013)	(0.013)	(0.014)
Means before lockdowns	23.281	23.281	23.281	64.824	64.824	64.824
Controls	Yes	Yes	Yes	Yes	Yes	Yes
Country and time FE	Yes	Yes	Yes	Yes	Yes	Yes
Observations	209,825	245,188	174,500	76,939	86,714	67,043

Notes: ***p < 0.01, **p < 0.05, *p < 0.1. Results of RDD using the optimal bandwidths based on Imbens and Kalyanaraman (2012). Clustered standard errors in parentheses are robust to within-day and within-country serial correlation. Control variables are daily temperature and rainfall (humidity for station-based data).

Table A3
COVID-19 lockdowns and air pollution − Other parameters of pollution.

Bandwidths	(1)	(2)	(3)
	Optimal bandwidth	Optimal bandwidth +10 days	Optimal bandwidth −10 days
Panel A: Air quality is measured by PM_{10}			
Lockdown = 1	−1.644**	−1.958***	−1.621**
	(0.739)	(0.676)	(0.722)
Means before lockdowns	30.655	30.655	30.655
Observations	83,886	92,890	74,209
Panel B: Air quality is measured by NO_2			
Lockdown = 1	−1.062***	−1.387***	−0.706*
	(0.349)	(0.326)	(0.374)
Means before lockdowns	12.880	12.880	12.880
Observations	65,473	75,076	55,942
Panel C: Air quality is measured by O_3			
Lockdown = 1	1.182***	1.554***	1.084***
	(0.360)	(0.337)	(0.356)
Means before lockdowns	14.543	14.543	14.543
Observations	51,809	60,682	42,850
Panel D: Air quality is measured by SO_2			
Lockdown = 1	−0.364*	−0.453**	−0.355
	(0.209)	(0.189)	(0.230)
Means before lockdowns	4.643	4.643	4.643
Observations	49,795	57,880	41,729
Controls	Yes	Yes	Yes
Country and time FE	Yes	Yes	Yes

Notes: ***p < 0.01, **p < 0.05, *p < 0.1. Results of RDD using the optimal bandwidths based on Imbens and Kalyanaraman (2012). The optimal bandwidths are 95, 76, 66 and 69 days for PM_{10}, NO_2, O_3, and SO_2, respectively. Clustered standard errors in parentheses are robust to within-day and within-country serial correlation. Control variables are daily temperature and humidity.

Table A4
COVID-19 lockdowns and air pollution – "Donut" RDD.

Bandwidth	Air pollution: NO_2			Air pollution: $PM_{2.5}$		
	Optimal bandwidth	Optimal bandwidth +10 days	Optimal bandwidth −10 days	Optimal bandwidth	Optimal bandwidth +10 days	Optimal bandwidth −10 days
Panel A: Excluding observations 5 days near the lockdown date						
Lockdown = 1	−1.641***	−1.955***	−1.215***	−3.781***	−3.841***	−3.486***
	(0.393)	(0.367)	(0.434)	(1.211)	(1.167)	(1.298)
Observations	234,913	277,840	192,349	73,810	83,727	63,848
Panel B: Excluding observations 10 days near the lockdown date						
Lockdown = 1	−2.120***	−2.408***	−1.554***	−3.948**	−4.079***	−3.615**
	(0.489)	(0.436)	(0.557)	(1.620)	(1.487)	(1.605)
Observations	214,381	257,308	171,817	69,467	79,384	59,505
Means before lockdowns	23.281	23.281	23.281	64.824	64.824	64.824
Controls	Yes	Yes	Yes	Yes	Yes	Yes
Country and time FE	Yes	Yes	Yes	Yes	Yes	Yes

Notes: ***p < 0.01, **p < 0.05, *p < 0.1. Results of "Donut" RDD using the optimal bandwidths based on Imbens and Kalyanaraman (2012). Clustered standard errors in parentheses are robust to within-day and within-country serial correlation. Control variables are daily temperature and rainfall (humidity for station-based data).

Table A5
COVID-19 lockdowns and air pollution – Alternative Optimal bandwidths.

Optimal bandwidth calculation method	Satellite NO_2		Station-based $PM_{2.5}$	
	CCT (Calonico, Cattaneo, and Titiunik)	Cross-valid (Lee and Lemieux)	CCT (Calonico, Cattaneo, and Titiunik)	Cross-valid (Lee and Lemieux)
Lockdown = 1	−1.125***	−1.224***	−0.558	−3.827***
	(0.305)	(0.325)	(1.010)	(1.191)
Optimal bandwidth	[-58, 76]	[-60, 60]	[-74, 109]	[-77, 77]
Means before lockdowns	23.281	23.281	64.824	64.824
Controls	Yes	Yes	Yes	Yes
Country and time FE	Yes	Yes	Yes	Yes
Observations	285,467	255,628	94,784	79,963

Notes: ***p < 0.01, **p < 0.05, *p < 0.1. Results of RDD using the optimal bandwidths based on Calonico et al. (2014) and Lee and Lemieux (2010). Clustered standard errors in parentheses are robust to within-day and within-country serial correlation. Control variables are daily temperature and rainfall (humidity for station-based data).

Table A6
COVID-19 lockdowns and air pollution − Alternative functional forms.

Panel A: Satellite air pollution Air quality:	Optimal bandwidth		Optimal bandwidth +10 days		Optimal bandwidth −10 days	
NO_2	(1)	(2)	(3)	(4)	(5)	(6)
Model 1: Cubic interaction model						
Lockdown = 1	−0.487**	0.377	−0.631***	−0.571***	−0.338	−0.294
	(0.241)	(0.305)	(0.220)	(0.221)	(0.264)	(0.264)
Model 2: Quartic interaction model						
Lockdown = 1	−1.058***	−1.242***	−1.193***	−1.032***	−0.939***	−0.832***
	(0.184)	(0.233)	(0.173)	(0.173)	(0.200)	(0.200)
Model 3: Quintic interaction model						
Lockdown = 1	−0.710***	−0.191	−0.851***	−0.754***	−0.534**	−0.469**
	(0.217)	(0.275)	(0.199)	(0.199)	(0.239)	(0.239)
Means before lockdowns	23.281	23.281	23.281	23.281	23.281	23.281
Controls	No	Yes	No	Yes	No	Yes
Country and time FE	Yes	Yes	Yes	Yes	Yes	Yes
Observations	260,007	257,339	303,316	300,266	216,917	214,775
Panel B: Station-based air pollution Air quality:	Optimal bandwidth		Optimal bandwidth +10 days		Optimal bandwidth −10 days	
$PM_{2.5}$	(1)	(2)	(3)	(4)	(5)	(6)
Model 1: Cubic interaction model						
Lockdown = 1	−1.155**	−0.427	−1.883***	−1.001*	0.320	0.869
	(0.579)	(0.621)	(0.548)	(0.592)	(0.620)	(0.659)
Model 2: Quartic interaction model						
Lockdown = 1	−3.819***	−2.021***	−4.156***	−2.233***	−3.386***	−1.573***
	(0.436)	(0.479)	(0.411)	(0.452)	(0.463)	(0.506)
Model 3: Quintic interaction model						
Lockdown = 1	−2.236***	−1.056*	−2.875***	−1.605***	−0.695	0.451
	(0.521)	(0.565)	(0.493)	(0.538)	(0.557)	(0.600)
Means before lockdowns	64.824	64.824	64.824	64.824	64.824	64.824
Controls	No	Yes	No	Yes	No	Yes
Country and time FE	Yes	Yes	Yes	Yes	Yes	Yes
Observations	90,938	79,200	100,869	89,117	80,962	69,238

Notes: ***p < 0.01, **p < 0.05, *p < 0.1. Results of RDD using the optimal bandwidths based on Imbens and Kalyanaraman (2012). The optimal bandwidths are 62 and 88 days for satellite and station-based data, respectively. Clustered standard errors in parentheses are robust to within-day and within-country serial correlation. Control variables are daily temperature and rainfall (humidity for station-based data).

Table A7
COVID-19 lockdowns and air pollution − RDD with additional covariates.

Bandwidth	Air pollution: NO_2			Air pollution: $PM_{2.5}$		
	Optimal bandwidth	Optimal bandwidth +10 days	Optimal bandwidth −10 days	Optimal bandwidth	Optimal bandwidth +10 days	Optimal bandwidth −10 days
Panel A: Controlling for pre-pandemic characteristics						
Lockdown = 1	−2.017***	−2.418***	−1.427**	−3.190**	−3.249**	−2.589*
	(0.599)	(0.502)	(0.609)	(1.524)	(1.437)	(1.565)
Country FE	No	No	No	No	No	No
Time FE	Yes	Yes	Yes	Yes	Yes	Yes
Means before lockdowns	23.281	23.281	23.281	64.824	64.824	64.824
Observations	185,307	215,912	154,577	73,693	82,986	64,434
Panel B: Controlling for country fixed-effects						
Lockdown = 1	−1.235***	−1.508***	−0.874**	−2.035*	−2.231*	−1.599
	(0.321)	(0.309)	(0.347)	(1.217)	(1.188)	(1.269)
Country FE	Yes	Yes	Yes	Yes	Yes	Yes

Table A7 (*continued*)

Bandwidth	Air pollution: NO_2			Air pollution: $PM_{2.5}$		
	Optimal bandwidth	Optimal bandwidth +10 days	Optimal bandwidth −10 days	Optimal bandwidth	Optimal bandwidth +10 days	Optimal bandwidth −10 days
Time FE	Yes	Yes	Yes	Yes	Yes	Yes
Means before lockdowns	23.281	23.281	23.281	64.824	64.824	64.824
Observations	257,339	300,266	214,775	79,200	89,117	69,238

Notes: ***p < 0.01, **p < 0.05, *p < 0.1. Results of RDD using the optimal bandwidths based on Imbens and Kalyanaraman (2012). The optimal bandwidths are 62 and 88 days for satellite and station-based data, respectively. Clustered standard errors in parentheses are robust to within-day and within-country serial correlation. Control variables in Panel A are daily temperature and rainfall (humidity for station-based data), log of GDP per capita (constant 2010 USD), population density, log of energy consumption per capita, motor vehicles per 1000 inhabitants, and share of electricity generated by coal power. Control variables in Panel B are daily temperature and rainfall (humidity for station-based data).

Table A8
COVID-19 lockdowns and air pollution - Weekly data.

Panel A: Satellite air pollution Air quality:	Optimal bandwidth		Optimal bandwidth +2 weeks		Optimal bandwidth −2 weeks	
NO_2	(1)	(2)	(3)	(4)	(5)	(6)
Model 1: Linear model						
Lockdown = 1	−1.033***	−1.004***	−1.549***	−1.559***	−0.629	−0.617
	(0.354)	(0.348)	(0.236)	(0.322)	(0.413)	(0.406)
Model 2: Linear interaction model						
Lockdown = 1	−0.986***	−0.938***	−1.507***	−1.513***	−0.567	−0.525
	(0.352)	(0.346)	(0.324)	(0.319)	(0.410)	(0.403)
Model 3: Quadratic model						
Lockdown = 1	−1.018***	−0.985***	−1.550***	−1.573***	−0.599	−0.571
	(0.352)	(0.347)	(0.325)	(0.320)	(0.411)	(0.404)
Model 4: Quadratic interaction model						
Lockdown = 1	−0.989***	−0.950***	−1.541***	−1.561***	−0.584	−0.566
	(0.358)	(0.352)	(0.329)	(0.323)	(0.420)	(0.412)
Means before lockdowns	23.281	23.281	23.281	23.281	23.281	23.281
Controls	No	Yes	No	Yes	No	Yes
Country and time FE	Yes	Yes	Yes	Yes	Yes	Yes
Observations	260,007	257,339	320,328	317,121	199,439	197,492
Panel B: Station-based air pollution Air quality:	Optimal bandwidth		Optimal bandwidth +2 weeks		Optimal bandwidth −2 weeks	
$PM_{2.5}$	(1)	(2)	(3)	(4)	(5)	(6)
Model 1: Linear model						
Lockdown = 1	−4.145***	−2.445*	−4.677***	−2.833**	−3.027**	−1.295
	(1.158)	(1.339)	(1.120)	(1.265)	(1.292)	(1.443)
Model 2: Linear interaction model						
Lockdown = 1	−3.387***	−1.842	−3.945***	−2.302*	−2.314*	−0.806
	(1.117)	(1.302)	(1.063)	(1.217)	(1.244)	(1.402)
Model 3: Quadratic model						
Lockdown = 1	−3.663***	−2.006	−4.261***	−2.513**	−2.572**	−0.964
	(1.127)	(1.317)	(1.078)	(1.233)	(1.254)	(1.418)
Model 4: Quadratic interaction model						
Lockdown = 1	−3.320***	−1.726	−3.936***	−2.172*	−2.141*	−0.623
	(1.104)	(1.287)	(1.058)	(1.209)	(1.238)	(1.381)
Means before lockdowns	64.824	64.824	64.824	64.824	64.824	64.824
Controls	No	Yes	No	Yes	No	Yes
Country and time FE	Yes	Yes	Yes	Yes	Yes	Yes
Observations	90,938	79,200	104,531	92,778	76,962	65,308

Notes: ***p < 0.01, **p < 0.05, *p < 0.1. Results of RDD using the optimal bandwidths based on Imbens and Kalyanaraman (2012). Clustered standard errors in parentheses are robust to within-day and within-country serial correlation. Model 1 uses running variable in linear form, Model 2 includes interaction of running variable and treatment variable, Model 3 includes quadratic term of running variable, Model 4 includes interactions of running variable (linear and quadratic terms) with treatment variable. Control variables are daily temperature and rainfall (humidity for station-based data).

Table A9
COVID-19 lockdowns and air pollution – 'Regular' stringency index.

Bandwidth	Air pollution: NO_2			Air pollution: $PM_{2.5}$		
	Optimal bandwidth	Optimal bandwidth +10 days	Optimal bandwidth −10 days	Optimal bandwidth	Optimal bandwidth +10 days	Optimal bandwidth −10 days
Lockdown = 1	−1.260***	−1.512***	−0.918***	−2.525**	−2.713**	−1.998
	(0.321)	(0.310)	(0.348)	(1.257)	(1.235)	(1.314)
Means before lockdowns	23.281	23.281	23.281	64.824	64.824	64.824
Controls	Yes	Yes	Yes	Yes	Yes	Yes
Country and time FE	Yes	Yes	Yes	Yes	Yes	Yes
Observations	257,339	300,266	214,775	79,200	89,117	69,238

Notes: ***p < 0.01, **p < 0.05, *p < 0.1. Results of RDD using the optimal bandwidths based on Imbens and Kalyanaraman (2012). Clustered standard errors in parentheses are robust to within-day and within-country serial correlation. Control variables are daily temperature and rainfall (humidity for station-based data). The 'regular' index returns null values if there are insufficient data to calculate the index while the 'display' version extrapolates to smooth over the last seven days of the index based on the most recent complete data. Our main analysis uses the 'display' version.

Table A10
Stringency index and air pollution – Principal Component Analysis.

Bandwidth	Air pollution: NO_2			Air pollution: $PM_{2.5}$		
	Optimal bandwidth	Optimal bandwidth +10 days	Optimal bandwidth −10 days	Optimal bandwidth	Optimal bandwidth +10 days	Optimal bandwidth −10 days
Lockdown = 1	−0.331**	−0.601***	−0.088	−2.570***	−3.115***	−1.401***
	(0.160)	(0.146)	(0.178)	(0.462)	(0.429)	(0.486)
Means before lockdowns	23.281	23.281	23.281	64.824	64.824	64.824
Controls	Yes	Yes	Yes	Yes	Yes	Yes
Country and time FE	Yes	Yes	Yes	Yes	Yes	Yes
Observations	260,241	300,811	218,404	79,623	89,384	69,921

Notes: ***p < 0.01, **p < 0.05, *p < 0.1. Results of RDD using the optimal bandwidths based on Imbens and Kalyanaraman (2012). Clustered standard errors in parentheses are robust to within-day and within-country serial correlation. Control variables are daily temperature and rainfall (humidity for station-based data). Stringency index is constructed using Principal Component Analysis. For all dimensions of stringency index, see Table B2 (Appendix B).

Table A11
Stringency index and air pollution – Alternative stringency indexes.

Bandwidth	Air pollution: NO_2		
	Optimal bandwidth	Optimal bandwidth +10 days	Optimal bandwidth −10 days
Panel A: Government response index			
Lockdown = 1	−1.360***	−1.850***	−1.237***
	(0.328)	(0.316)	(0.356)
Observations	256,082	299,211	213,210
Panel B: Containment and health index			
Lockdown = 1	−1.444***	−1.943***	−1.334***
	(0.328)	(0.316)	(0.356)
Observations	256,078	299,181	213,353
Panel C: Economic support index			
Lockdown = 1	0.499*	0.558**	0.342
	(0.255)	(0.245)	(0.285)
Observations	249,421	281,210	213,744

Table A11 (*continued*)

Bandwidth	Air pollution: NO_2		
	Optimal bandwidth	Optimal bandwidth +10 days	Optimal bandwidth −10 days
Means before lockdowns	23.281	23.281	23.281
Controls	Yes	Yes	Yes
Country and time FE	Yes	Yes	Yes

Notes: ***p < 0.01, **p < 0.05, *p < 0.1. Results of RDD using the optimal bandwidths based on Imbens and Kalyanaraman (2012). Clustered standard errors in parentheses are robust to within-day and within-country serial correlation. All indexed are taken from "display" version of OxCGRT which will extrapolate to smooth over the last seven days of the index based on the most recent complete data. All regressions include country dummies and week dummies. Control variables are daily temperature and rainfall.

Table A12
COVID-19 lockdowns and air pollution − Country linear time trend.

Bandwidth	Air pollution: NO_2			Air pollution: $PM_{2.5}$		
	Optimal bandwidth	Optimal bandwidth +10 days	Optimal bandwidth −10 days	Optimal bandwidth	Optimal bandwidth +10 days	Optimal bandwidth −10 days
Model 1: Linear model						
Lockdown = 1	−1.176***	−1.510***	−0.953***	−2.877**	−2.941**	−2.357*
	(0.330)	(0.313)	(0.352)	(1.244)	(1.242)	(1.301)
Model 2: Linear interaction model						
Lockdown = 1	−1.133***	−1.488***	−0.901**	−2.386*	−2.515**	−1.941
	(0.328)	(0.310)	(0.350)	(1.218)	(1.203)	(1.271)
Model 3: Linear interaction model						
Lockdown = 1	−1.158***	−1.516***	−0.919***	−2.469**	−2.629**	−2.018
	(0.329)	(0.310)	(0.350)	(1.231)	(1.216)	(1.286)
Model 4: Quadratic interaction model						
Lockdown = 1	−1.137***	−1.501***	−0.903**	−2.376*	−2.465**	−1.963
	(0.330)	(0.312)	(0.351)	(1.212)	(1.196)	(1.262)
Means before lockdowns	23.281	23.281	23.281	64.824	64.824	64.824
Controls	Yes	Yes	Yes	Yes	Yes	Yes
Country and time FE	Yes	Yes	Yes	Yes	Yes	Yes
Country linear time trend	Yes	Yes	Yes	Yes	Yes	Yes
Observations	257,339	300,266	214,775	79,200	89,117	69,238

Notes: ***p < 0.01, **p < 0.05, *p < 0.1. Results of RDD using the optimal bandwidths based on Imbens and Kalyanaraman (2012). The optimal bandwidths are 62 and 88 days for satellite and station-based data, respectively. Clustered standard errors in parentheses are robust to within-day and within-country serial correlation. Model 1 uses running variable in linear form, Model 2 includes interaction of running variable and treatment variable, Model 3 includes quadratic term of running variable, Model 4 includes interactions of running variable (linear and quadratic terms) with treatment variable. Control variables are daily temperature and rainfall (humidity for station-based data).

Table A13
COVID-19 lockdowns and air pollution − Air pollution in log form.

Bandwidth	Air pollution: NO_2			Air pollution: $PM_{2.5}$		
	Optimal bandwidth	Optimal bandwidth +10 days	Optimal bandwidth −10 days	Optimal bandwidth	Optimal bandwidth +10 days	Optimal bandwidth −10 days
Model 1: Linear model						
Lockdown = 1	−0.035***	−0.044***	−0.026**	−0.054***	−0.042**	−0.051***
	(0.011)	(0.010)	(0.012)	(0.019)	(0.018)	(0.019)
Model 2: Linear interaction model						
Lockdown = 1	−0.034***	−0.043***	−0.023**	−0.050***	−0.038**	−0.048**
	(0.011)	(0.010)	(0.012)	(0.019)	(0.018)	(0.019)
Model 3: Linear interaction model						
Lockdown = 1	−0.035***	−0.044***	−0.024**	−0.051***	−0.039**	−0.049**
	(0.011)	(0.010)	(0.012)	(0.019)	(0.018)	(0.019)

(*continued on next page*)

Table A13 (*continued*)

Bandwidth	Air pollution: NO_2			Air pollution: $PM_{2.5}$		
	Optimal bandwidth	Optimal bandwidth +10 days	Optimal bandwidth −10 days	Optimal bandwidth	Optimal bandwidth +10 days	Optimal bandwidth −10 days
Model 4: Quadratic interaction model						
Lockdown = 1	−0.033***	−0.043***	−0.023**	−0.050***	−0.037**	−0.048**
	(0.011)	(0.010)	(0.012)	(0.019)	(0.018)	(0.019)
Means before lockdowns	23.281	23.281	23.281	64.824	64.824	64.824
Controls	Yes	Yes	Yes	Yes	Yes	Yes
Country and time FE	Yes	Yes	Yes	Yes	Yes	Yes
Observations	254,477	297,076	212,387	79,200	89,117	69,238

Notes: ***p < 0.01, **p < 0.05, *p < 0.1. Results of RDD using the optimal bandwidths based on Imbens and Kalyanaraman (2012). The optimal bandwidths are 62 and 88 days for satellite and station-based data, respectively. Clustered standard errors in parentheses are robust to within-day and within-country serial correlation. Model 1 uses running variable in linear form, Model 2 includes interaction of running variable and treatment variable, Model 3 includes quadratic term of running variable, Model 4 includes interactions of running variable (linear and quadratic terms) with treatment variable. Control variables are daily temperature and rainfall (humidity for station-based data).

Table A14
Heterogeneity analysis.

Air quality: NO_2	Optimal bandwidth	Optimal bandwidth +10 days	Optimal bandwidth −10 days
	(1)	(2)	(3)
Panel A: Location			
Lockdown*Countries near equator	3.543***	3.785***	3.106***
	(0.308)	(0.279)	(0.327)
Observations	257,339	300,266	214,775
Panel B: Democracy			
Reference: Authoritarian			
Lockdown*Hybrid regime	1.432**	1.328**	1.284**
	(0.572)	(0.546)	(0.589)
Lockdown*Partial democracy	1.197**	1.513***	0.877
	(0.557)	(0.518)	(0.589)
Lockdown*Full democracy	0.469	−0.015	−0.264
	(0.855)	(0.851)	(0.916)
Observations	233,029	271,501	194,642
Panel C: Share of trade			
Lockdown*Trade	−0.034***	−0.033***	−0.039***
	(0.012)	(0.010)	(0.014)
Observations	199,787	232,666	167,163
Panel D: Share of manufacturing			
Lockdown*Manufacturing	−0.439***	−0.454***	−0.482***
	(0.052)	(0.050)	(0.056)
Observations	172,872	201,016	144,775
Panel E: Air pollution index			
Reference: 1st quintile			
Lockdown*2nd quintile	1.005**	0.978*	0.772
	(0.511)	(0.510)	(0.567)
Lockdown*3rd quintile	1.602***	1.826***	1.575***
	(0.476)	(0.466)	(0.538)
Lockdown*4th quintile	−0.716	−1.134*	−0.811
	(0.619)	(0.606)	(0.666)
Lockdown*5th quintile	−0.577	−0.643	−0.755
	(0.663)	(0.636)	(0.726)
Observations	254,146	296,573	212,140
Means before lockdowns	23.281	23.281	23.281
Controls	Yes	Yes	Yes
Country and time FE	Yes	Yes	Yes

Notes: ***p < 0.01, **p < 0.05, *p < 0.1. Results of RDD using the optimal bandwidths based on Imbens and Kalyanaraman (2012). The optimal bandwidths are 62 and 88 days for satellite and station-based data, respectively. Clustered standard errors in parentheses are robust to within-day and within-country serial correlation. Control variables are daily temperature and rainfall (humidity for station-based data).

Appendix B. Data Sources

To examine the relationship between COVID-19 and air quality, we use two measures of air pollution, namely fine particulate matter $PM_{2.5}$ (mass concentration of particles with diameters $\leq$2.5 μm) and nitrogen dioxide NO_2. While other pollutants are available in our dataset, we select the $PM_{2.5}$ and NO_2 given their direct link to human health. $PM_{2.5}$ is a common cause for adverse health outcomes such as chronic obstructive pulmonary disease (COPD) and lower respiratory infection (LRI) causing death of nearly three million people globally (Gakidou et al., 2017). At the same time, NO_2 is the leading source of childhood asthma in urban areas globally (Achakulwisut et al., 2019). In this study, we collect data on these measures from October 1st, 2019 to June 1st, 2020. We also use other pollutants, such as PM_{10}, SO_2 and O_3, for robustness checks.

The NO_2 data are derived from images of pollution-monitoring satellites released by the National Aeronautics and Space Administration (NASA) and European Space Agency (ESA). In particular, we use data from the Sentinel-5P/TROPOMI (S5P) instrument of the European Union's Copernicus programme. The Copernicus S5P provides daily global coverage of atmospheric parameters at high resolution (i.e., a pixel size of about 5.5 km $\times$ 3.5 km after August 6th, 2019).[11] We then use Google Earth Engine to process and average air quality data at the sub-national level using administrative areas from Database of Global Administrative Areas (GADM). In particular, we measure air pollution at the first-order administrative division (ADM1).[12] While the Copernicus S5P records a wide range of pollutants including NO_2 and others (O_3, SO_2, CO, CH_4, and aerosols), we focus on NO_2 because this is a noxious gas emitted by motor vehicles, power plants, and industrial facilities (see, e.g., Dutheil et al. (2020)). Among other pollutants, NO_2 is also a particularly well-suited data to analysis of emission because it has a short lifetime; this implies that molecules of NO_2 stay fairly close to their sources and thus offer an appropriate measure of changes in emissions.

A potential concern of using satellite air quality, however, is cloud cover. This can bias results by obscuring the sensor's view of the lower atmosphere. Concentrations of NO_2 in the atmosphere are also highly variable in space and time due to factors such as varying traffic flows on weekdays versus weekends and changes in weather conditions. Therefore, we follow suggestions from the Copernicus program and perform a cloud masking which excludes results from pixels with >10 percent cloud fraction.[13] We also average data over weekly periods as a robustness test. Finally, we include data on daily rainfall and temperature to control for weather conditions, which are derived from the National Center for Environmental Prediction (NCEP) at the National Oceanic and Atmospheric Administration (NOAA). The global dataset provides four 6-h daily records of temperature and precipitation at the resolution of approximately 25 km. We extract the weather data at the sub-national level using a similar process as with the air pollution data.

As an alternative measure of air quality, we use daily station-based air quality index (AQI) from the World Air Quality Index (WAQI) project. The AQI provides accurate and reliable information on different air pollutant species from more than 12,000 ground-based air quality monitoring stations (primarily located at/near the US embassies and consulates) situated in 1000 major cities in more than 100 countries from 2014 to present. However, there are certain limitations with station-based data. One is that station-based data are often reported more slowly, and not in a 'real-time' fashion as satellite data. Another limitation is the locations of air quality monitoring stations are likely not random, so they may not provide representative data on an area's air quality. Consequently, the satellite data are our preferred data for analysis.

We subsequently match the air pollution data with the government stringency data from the Oxford COVID-19 Government Response Tracker (OxCGRT). The OxCGRT is a novel country-level dataset published by the Blavatnik School of Government at the University of Oxford, which contains information on various lockdown measures, such as school and workplace closings, travel restrictions, bans on public gatherings, and stay-at-home requirements (Hale et al., 2020). It measures government stringency responses on a scale of 0—100. We provide a description of the index components in Table B2 (Appendix B).

To explore a potential channel through which COVID-19 affects air quality, we collect data on mobility from Google Community Mobility Reports. The Google Community Mobility Reports provide daily data on Google Maps users who have opted-in to the 'location history' in their Google accounts settings across 132 countries. The reports calculate changes in movement compared to a baseline, which is the median value for the corresponding day of the week from January to present. The purpose of travel has been assigned to one of the following categories: retail and recreation, groceries and pharmacies, parks, transit stations, workplaces, and residential. In our analysis, we expect that the lockdowns will lead to reduced mobility of all categories, except for the residential category. We also examine data from several additional sources for robustness checks. The data sources are listed in Table B1 (Appendix B).

[11] The data have recently been used to study changes in air quality caused by COVID-19 in some health and environmental studies (see, e.g., Chen et al. (2020) and Zambrano-Monserrate et al. (2020)).

[12] In some countries, the ADM1 refers to province level while for others, it refers to state/region level. The administrative data are available at https://gadm.org/about.html.

[13] For more details, see: https://atmosphere.copernicus.eu/flawed-estimates-effects-lockdown-measures-air-quality-derived-satellite-observations?q=flawed-estimates-effects-lockdown-measures-air-quality-satellite-observations.

Table B1
Data sources and summary statistics.

Variable	Descriptions	Mean	Standard deviation	Min	Max
Oxford COVID-19 Government Response Tracker (OxCGRT)					
Source: Blavatnik School of Government at the University of Oxford (https://covidtracker.bsg.ox.ac.uk/)					
Stringency index	Government responses to COVID-19 (Score between 0 and 100)	44.751	35.254	0	100
Government response index		41.404	31.499	0	96.15
Containment and health index		44.148	33.202	0	100
Economic support index		26.331	32.501	0	100
Satellite air quality (daily)					
Source: European Union's Copernicus programme (https://sentinels.copernicus.eu/web/sentinel/missions/sentinel-5p)					
NO_2	Nitrogen dioxide	20.458	26.334	−43.400	886
Satellite weather data (daily)					
Source: National Oceanic and Atmospheric Administration (NOAA) (https://www.ncep.noaa.gov)					
Rainfall	Average rainfall (m)	0.0002	0.0003	0.000	0.015
Temperature	Average temperature (K)	289.715	10.399	232.625	313.183
Station-based data (daily)					
Source: World Air Quality Index (WAQI) project (https://waqi.info/)					
$PM_{2.5}$	Particles with a diameter of 2.5 μm or less	56.291	43.799	1	999
PM_{10}	Particles with a diameter of 10 μm or less	27.338	25.403	1	999
NO_2	Nitrogen dioxide	10.118	8.442	0	500
SO_2	Sulfur dioxide	4.126	7.895	0	500
O_3	Ozone	19.459	12.670	0	500
Humidity	Average humidity (percent)	69.084	19.276	0	122
Temperature	Average temperature (°C)	14.393	9.200	−67.7	93.3
Mobility rates					
Source: Google Community Mobility Reports (https://www.google.com/covid19/mobility/)					
Retail & Recreation	Changes in people's mobility (percent) in different categories	−22.801	28.661	−100	313
Grocery & pharmacy		−6.118	21.645	−100	345
Park		−2.925	51.956	−100	616
Transit		−27.151	30.046	−100	497
Workplaces		−23.812	21.033	−94	258
Residential		10.669	9.177	−25	56
Other control variables (Table A7)					
Source: World Bank World Development Indicators (https://databank.worldbank.org/source/world-development-indicators)					
Energy consumption	Energy consumption per capita (kWh)	24,620	25,452	706.246	215,883
Vehicles	Number of motor vehicles per 1000 inhabitants	200.713	217.914	1.000	797
GDP	GDP per capita (in constant 2010 USD)	13,260	17,763	208.075	111062
Population density	People per sq. km of land area	164.668	586.711	0.137	20480
CO2 emissions	CO2 emissions (kg per 2010 US$ of GDP)	0.516	0.374	0.056	2.004
Electricity	Electricity production from coal sources (percent of total)	19.917	24.166	0.000	96.360
Other control variables (Table A14)					
Democracy index	2019 Economist Intelligence Unit Report (https://www.eiu.com/topic/democracy-index)	54.714	20.579	13.200	98.700
Air index	2018 WHO Global Ambient Air Quality Database (https://www.who.int/airpollution/data)	36.234	31.953	4.071	203.744
Manufacturing	Share of manufacturing in GDP (*2019 World Development Indicators database*)	12.937	5.892	1.686	30.838
Trade	Share of trade in GDP (*2019 World Development Indicators database*)	90.162	54.906	26.722	381.517

Table B2
Stringency index components.

Number	Components	Description
1	School closing	Record closings of schools and universities
2	Workplace closing	Record closings of workplaces
3	Cancel public events	Record cancelling public events
4	Restrictions on gatherings	Record the cut-off size for bans on private gatherings
5	Close public transport	Record closing of public transport
6	Stay at home requirements	Record orders to "shelter-in- place" and otherwise confine to home
7	Restrictions on internal movement	Record restrictions on internal movement
8	International travel controls	Record restrictions on international travel
9	Public info campaigns	Record presence of public info campaigns

Notes: Each component is measured by an ordinal scale. The stringency index is measured by the OxCGRT team as simple averages of the individual component indicators. Each component is measured by an ordinal scale (e.g. 0 − no measures, 1 − recommended closing, 2 − require partial closing, 3 − require closing all levels). It is then rescaled by maximum value to create a score between 0 and 100. These scores are then averaged to get the stringency index.

Appendix C. Further robustness checks and heterogeneity analysis

Further robustness checks

To further check the robustness of our findings, we conduct a battery of tests on the estimation results. These include employing different methods of calculating the optimal bandwidth, higher-degree polynomials of the running variable, adding different covariates to the regressions, using wider time bandwidths and different thresholds and versions of the stringency index, controlling for potentially differential time trends across countries, and converting the air quality variables into logarithmic form.

First, our main analysis applies the optimal bandwidth choice rule of Imbens and Kalyanaraman (2012) to select the optimal bandwidth to minimize mean-squared error. In Table A5 (Appendix A), we report the results using alternative methods including CCT (Calonico et al., 2014) and Cross-valid (Lee and Lemieux, 2010).[14] We find consistent impacts of the lockdowns on NO_2 using the satellite data and $PM_{2.5}$ using the alternative station-based data. We also check the robustness of our results by using high-order polynomial of the running variable. Our results are generally consistent, as presented in Table A6 (Appendix A). Still, we note that controlling for high-order polynomials in regression discontinuity analysis may lead to noisy estimates of the impact of lockdown (Gelman and Imbens, 2019).

Second, our estimation results are rather similar whether we control for weather conditions in our RDD regressions. For further checks, we include additional covariates to control for the pre-pandemic country characteristics, namely country's log of GDP per capita (in constant 2010 USD), population density, log of energy consumption per capita, the number of motor vehicles per 1000 inhabitants, and the share of electricity generated by coal power. These country characteristics come from the World Development Indicators (WDI) database in the latest year when data is available. We present the estimation results in panel A of Table A7 (Appendix A) and we also provide the main results with country fixed effects in Panel B for comparison purpose. Our main findings remain robust to the inclusion of additional covariates.

Third, a potential issue with daily air pollution data is that these data can substantially vary from one day to another because of variations in emission and changes in weather conditions. Therefore, we replicate our RDD approach using a weekly indicator. We employ the optimal bandwidths selection and find that the results are generally consistent with the main findings in Table 2 (see Table A8, Appendix A).

Fourth, we use alternative measures of stringency index taken from the OxCGRT dataset. There are two versions of the stringency index: (i) a "regular" version which returns null values if there are insufficient data to calculate the index, and (ii) a "display" version which extrapolates to smooth over the last seven days of the index based on the most recent complete data. We use the latter indicator for our main analysis, but we also find consistent results using the "regular" version (Appendix A, Table A9).

Fifth, the stringency index in the OxCGRT dataset is calculated using a simple additive unweighted approach. It is thus possible that some dimensions with higher weights will be underestimated in the index. To address this issue, we create a new index based on the Principal Component Analysis (PCA) method for all the dimensions of stringency index. Table A10 in Appendix A shows rather similar estimation results for our own index, except for the optimal bandwidth −10 days (column 3).

[14] We apply the user-written program "*rdbwselect*" provided by Calonico et al. (2014) to estimate the cross-validation functions that determine our bandwidths.

Sixth, we further explore other indexes that are available from the OxCGRT dataset. They include: (i) Government response index, (ii) Containment and health index, and (iii) Economic support index.[15] Compared to our main measure, the government response index and the containment and health index include two additional dimensions: testing policy and contact tracing. Still, we find a consistent impact of the lockdowns on air pollution when using these indexes, except for the economic support index (Appendix A, Table A11). However, the economic support index only includes income support programs and debt relief programs, so it does not fully capture the overall responsiveness of the government.

We also check whether our results are driven by differential time trends across countries. We include in the regressions the interaction terms of country dummies with linear time trends. The results, presented in Table A12 (Appendix A), are generally consistent with our main findings. Finally, our findings also remain consistent when we use the logarithmic form of the air quality variable (Appendix A, Table A13).

Heterogeneity analysis

Having shown that changes in air quality are driven by COVID-19, it is useful to understand whether the impacts of lockdowns differ by certain country characteristics. In particular, the impacts of lockdowns can vary according to a country's geographic location. For example, cities near the deserts are often affected by sand and dust storms, which can strongly impact air quality. We thus interact a dummy variable indicating whether a country is near the equator with the treatment variable. The results presented in panel A of Table A14 (Appendix A) show that countries near the equator have a higher concentration of NO_2 after the lockdowns.

A country's institution may also affect the impacts of lockdowns. A large body of economic literature has shown the important role of institutions and culture in shaping economic development (e.g. Gorodnichenko and Roland, 2017; Acemoglu et al., 2019). Consequently, we use the democracy index from the 2019 report of the Economist Intelligence Unit. We expect that countries with strong institutions likely implement stringent policies during the time of COVID-19, and therefore have a better performance in terms of air quality. The results in panel B of Table A14 (Appendix A), however, provide little support for this argument. In contrast, partial democratic countries and countries with hybrid regime appear to have less reduced air pollution after the lockdowns than authoritarian countries.

Another useful heterogeneity analysis is whether countries with a high level of openness have more reduced air pollution after the lockdowns. Whether trade is good or bad for the environment has been a topic of debate in the literature. While evidence exists on the beneficial effects of trade on the environment (e.g. Antweiler et al., 2001; Frankel and Rose, 2005), other studies show that trade openness could in fact lead to higher emissions (Managi et al., 2009; Li et al., 2015). To answer this question, we interact a country's share of manufacturing and share of trade in its GDP (from the 2019 World Development Indicators (WDI) database) with the treatment variable. The estimation results, presented in panels C and D of Table A14 (Appendix A), show that countries with a larger share of trade or manufacturing have more reduced air pollution after the lockdowns.

Finally, we examine whether countries with existing lower levels of air pollution may reduce air pollution more. We use the WHO Global Ambient Air Quality Database that summarizes concentration of $PM_{2.5}$ at the country level in 2018. We then split our sample into five quintiles and interact each with our treatment variable. The results in panel E indicate that countries with an initially lower level of air pollution (i.e., the 1st quintile) have more reduced air pollution compared to those with initially higher levels of air pollution. For further illustration, we interact our treatment variable with the country dummies and plot the estimated interaction terms against countries' initial level of air quality in Figure A5 (Appendix A). We highlight a country's population size by drawing a bubble graph, where the size of a country's circle is proportionate to its population size. Figure A5 shows countries bunching to the left of the graph and below the zero (no change) line, confirming that countries with better air quality before the pandemic tend to have higher reduction of NO_2. Several countries with a large population size that improved air quality stand out, including China, Iraq, Norway, Russia, South Korea, and the United States.

References

Achakulwisut, P., Brauer, M., Hystad, P., Anenberg, S.C., 2019. Global, national, and urban burdens of paediatric asthma incidence attributable to ambient NO2 pollution: estimates from global datasets. Lancet Planetary Health 3 (4), e166–e178.
Akesson, J., Ashworth-Hayes, S., Hahn, R., Metcalfe, R.D., Rasooly, I., 2020. Fatalism, Beliefs, and Behaviors during the COVID-19 Pandemic (No. W27245). National Bureau of Economic Research.
Almond, D., Du, X., Zhang, S., 2020. Did COVID-19 Improve Air Quality Near Hubei? (No. W27086). National Bureau of Economic Research.
Anderson, M.L., 2014. Subways, strikes, and slowdowns: the impacts of public transit on traffic congestion. Am. Econ. Rev. 104 (9), 2763–2796.
Auffhammer, M., Kellogg, R., 2011. Clearing the air? The effects of gasoline content regulation on air quality. Am. Econ. Rev. 101 (6), 2687–2722.
Baker, S.R., Farrokhnia, R.A., Meyer, S., Pagel, M., Yannelis, C., 2020. How Does Household Spending Respond to an Epidemic? Consumption during the 2020 Covid-19 Pandemic (No. W26949). National Bureau of Economic Research.
Barreca, A.I., Guldi, M., Lindo, J.M., Waddell, G.R., 2011. Saving babies? Revisiting the effect of very low birth weight classification. Q. J. Econ. 126 (4), 2117–2123.
Brodeur, A., Cook, N., Wright, T., 2020. On the Effects of COVID-19 Safer-At-Home Policies on Social Distancing, Car Crashes and Pollution (No. 13255). IZA Discussion Paper.
Brunekreef, B., Holgate, S.T., 2002. Air pollution and health. Lancet 360 (9341), 1233–1242.

[15] Another index is Legacy stringency index; however, it is not recommended by the OxCGRT team (Hale et al., 2020).

Calonico, S., Cattaneo, M.D., Titiunik, R., 2014. Robust nonparametric confidence intervals for regression-discontinuity designs. Econometrica 82 (6), 2295–2326.
Chen, Y., Whalley, A., 2012. Green infrastructure: the effects of urban rail transit on air quality. Am. Econ. J. Econ. Pol. 4 (1), 58–97.
Cicala, S., Holland, S.P., Mansur, E.T., Muller, N.Z., Yates, A.J., 2020. Expected Health Effects of Reduced Air Pollution from COVID-19 Social Distancing (No. W27135). National Bureau of Economic Research.
Cole, M., Ozgen, C., Strobl, E., 2020. Air Pollution Exposure and COVID-19 (No. 13367) (IZA Discussion Paper).
Dang, H.A.H., Nguyen, C.V., 2020. Gender Inequality during the COVID-19 Pandemic: Income, Expenditure, Savings, and Job Loss. World Development, p. 105296.
Davis, L.W., 2008. The effect of driving restrictions on air quality in Mexico City. J. Polit. Econ. 116 (1), 38–81.
Fairlie, R.W., Couch, K., Xu, H., 2020. The Impacts of COVID-19 on Minority Unemployment: First Evidence from April 2020 CPS Microdata (No. W27246). National Bureau of Economic Research.
Gakidou, E., Afshin, A., Abajobir, A.A., Abate, K.H., Abbafati, C., Abbas, K.M., Abu-Raddad, L.J., 2017. Global, regional, and national comparative risk assessment of 84 behavioural, environmental and occupational, and metabolic risks or clusters of risks, 1990–2016: a systematic analysis for the Global Burden of Disease Study 2016. Lancet 390 (10100), 1345–1422.
Gelman, A., Imbens, G., 2019. Why high-order polynomials should not be used in regression discontinuity designs. J. Bus. Econ. Stat. 37 (3), 447–456.
Hahn, J., Todd, P., Van der Klaauw, W., 2001. Identification and estimation of treatment effects with a regression-discontinuity design. Econometrica 69 (1), 201–209.
Hale, T., Petherick, A., Phillips, T., Webster, S., 2020. Variation in Government Responses to COVID-19 (No. 31) (Blavatnik School of Government working paper).
Hausman, C., Rapson, D.S., 2018. Regression discontinuity in time: considerations for empirical applications. Ann. Rev. Resour. Econ. 10, 533–552.
He, G., Pan, Y., Tanaka, T., 2020. The short-term impacts of COVID-19 lockdown on urban air pollution in China. Nat. Sustain. https://doi.org/10.1038/s41893-020-0581-y.
Imbens, G., Kalyanaraman, K., 2012. Optimal bandwidth choice for the regression discontinuity estimator. Rev. Econ. Stud. 79 (3), 933–959.
Isphording, I.E., Pestel, N., 2020. Pandemic Meets Pollution: Poor Air Quality Increases Deaths by COVID-19. (No. 13418) (IZA Discussion Paper).
Lee, D.S., Lemieux, T., 2010. Regression discontinuity designs in economics. J. Econ. Lit. 48 (2), 281–355.
Lenzen, M., Li, M., Malik, A., Pomponi, F., Sun, Y.Y., Wiedmann, T., et al., 2020. Global socio-economic losses and environmental gains from the Coronavirus pandemic. PloS One 15 (7), e0235654.
Liu, C., Chen, R., Sera, F., Vicedo-Cabrera, A.M., Guo, Y., Tong, S.,, et al., 2019. Ambient particulate air pollution and daily mortality in 652 cities. N. Engl. J. Med. 381 (8), 705–715.
Smith, L.V., Tarui, N., Yamagata, T., 2020. Assessing the Impact of COVID-19 on Global Fossil Fuel Consumption and CO2 Emissions (No. 202016). University of Hawaii at Manoa, Department of Economics.
Tobías, A., Carnerero, C., Reche, C., Massagué, J., Via, M., Minguillón, M.C., Alastuey, A., Querol, X., 2020. Changes in air quality during the lockdown in Barcelona (Spain) one month into the SARS-CoV-2 epidemic. Sci. Total Environ. 138540.
Venter, Z.S., Aunan, K., Chowdhury, S., Lelieveld, J., 2020. COVID-19 lockdowns cause global air pollution declines. In: Proceedings of the National Academy of Sciences, p. 202006853.
Viard, V.B., Fu, S., 2015. The effect of Beijing's driving restrictions on pollution and economic activity. J. Publ. Econ. 125, 98–115.

References

Chen, K., Wang, M., Huang, C., Kinney, P.L., Anastas, P.T., 2020. Air pollution reduction and mortality benefit during the COVID-19 outbreak in China. Lancet Planetary Health 4 (6), e210–e212.
Dutheil, F., Baker, J.S., Navel, V., 2020. COVID-19 as a factor influencing air pollution? Environ. Pollut. 263, 114466.
Zambrano-Monserrate, M.A., Ruano, M.A., Sanchez-Alcalde, L., 2020. Indirect effects of COVID-19 on the environment. Sci. Total Environ. 138813.
Acemoglu, D., Naidu, S., Restrepo, P., Robinson, J.A., 2019. Democracy does cause growth. J. Polit. Econ. 127 (1), 47–100.
Antweiler, W., Copeland, B.R., Taylor, M.S., 2001. Is free trade good for the environment? Am. Econ. Rev. 91 (4), 877–908.
Frankel, J.A., Rose, A.K., 2005. Is trade good or bad for the environment? Sorting out the causality. Rev. Econ. Stat. 87 (1), 85–91.
Gorodnichenko, Y., Roland, G., 2017. Culture, institutions, and the wealth of nations. Rev. Econ. Stat. 99 (3), 402–416.
Li, Z., Xu, N., Yuan, J., 2015. New evidence on trade-environment linkage via air visibility. Econ. Lett. 128, 72–74.
Managi, S., Hibiki, A., Tsurumi, T., 2009. Does trade openness improve environmental quality? J. Environ. Econ. Manag. 58 (3), 346–363.